Strain-induced electronic property heterogeneity of a carbon nanotube

D. Tekleab and D. L. Carroll
Department of Physics and Astronomy, Clemson University, Kinard Laboratory of Physics, Clemson, South Carolina 29634

G. G. Samsonidze and B. I. Yakobson
Mechanical Engineering and Materials Science Department and Center for Nanoscale Science and Technology, Rice University, Houston, Texas 77005-1892

(Received 2 January 2001; published 27 June 2001)

We have studied the effect of strain on the electronic properties of multiwall carbon nanotubes using scanning tunneling microscopy and spectroscopy. While small elastic strain causes no change of the electronic properties of the nanotubes, tubes under large strain by lying over an inter-grain boundary of the Au substrate show drastic electronic heterogeneity. The observed variation in local electronic property is explained in terms of the mechanical relaxation of the outer most layer of the tube. This provides first evidence of the effect of mechanical modification on local electronic structure of a carbon nanotube.

DOI: 10.1103/PhysRevB.64.035419 PACS number(s): 61.48.+c, 68.37.Ef

Carbon nanotubes have attracted much attention due to their unique mechanical and electrical properties. They are extremely strong fibers.[1] Their electrical properties are dictated by their geometry, e.g., metallic or semiconducting depending on their diameter and chirality.[2–4] Unusually, however, deformations of the tubes affect their electronic properties. Depending on the magnitude of loading and the morphologies of the substrates on which they are deposited, tubes can be deformed to various degrees, which may include flattening, bending, kinking, or twisting. These deformations break the tube symmetry, and a change in their electronic properties should result.[5–8] Radial deformation of armchair tubes (flattening), for example, breaks mirror symmetry causing the tube to develop a pseudogap as a result of π-π^* hybridization.[6] In transport measurements tubes bend as they tend to adhere to the substrate and the contacting electrodes leading to high values in the measured contact resistance.[7,9,10] Empirical tight-binding studies also suggest that external influences such as axial tensile stress contribute to band-gap modifications.[11] These reports further predict that nanotubes may undergo local metal-insulator transition due to axial strains.

Clearly, such strains must lead to mechanical relaxation of the lattice and this has been addressed theoretically.[12–14] Mechanical relaxation in these strongest materials takes place through successive Stone-Wale's bond rotations. Such mechanical relaxation can cause local changes both in the chirality and the diameter of the tube, which leads to local change in electronic property. Despite extensive theoretical studies on the relation between the mechanical and electrical properties of the tubes, no direct measurement yet exists to verify the theoretical predictions. Here we report to the best of our knowledge, on the first evidence of the possible relation between mechanical modification and local electronic structure of carbon nanotubes. The close relationship between the mechanical and electronic properties makes nanotubes particularly suitable for building carbon nanotube based electronic devices.

In these experiments arc-grown multiwalled nanotubes (MWNT) were dispersed in tetrahydrofuran using ultrasonication. For scanning tunneling microscopy (STM) studies, a few drops of solution were deposited on an initially cleaned Au substrate. This sample was then transferred into a prechamber where the solvent was pumped away before being introduced into ultrahigh vacuum. The substrate containing the sample is then heated to insure that influences due to surface adsorbates are minimized. STM imaging and current-voltage (I-V) spectroscopies were performed at 1×10^{-10} Torr using Pt-Ir tips. Imaging set points were typically 100 mV at 20 pA.

STM/STS results performed on two tubes, one under small strain ($T1$) and one under large strain ($T2$) are shown in Figs. 1 and 2. Figures 1(a) and 1(b) are STM images of $T1$ on a clean Au substrate. The tube is located to the left of the dashed line on a flat surface. The region to the right of the tube is an imaging artifact. Such artifacts arise during STM imaging of tubes from the double tip effect.[15] The tube is bent and is held fixed to the substrate by van der Waals forces from the substrate. The bends on $T1$ are not as abrupt as in previously reported tube bends/kinks.[5,16–18] The height profile versus horizontal distance curves (not shown) of the tube are smooth suggesting no abrupt structural deformation or damage exists on the tube. The diameter of the tube is 12.0 nm$\pm$0.5 nm and the radius of curvature in the lower bent section of the tube is $\sim$300 nm. A rough estimate of the strain on the tube yields $\varepsilon = d/2R \sim 0.02$, where d is the diameter of the tube and R is the radius of curvature respectively.

The recorded spectroscopy (I-V) data from the locations marked $a-c$ in Fig. 1(b) was used to compute the corresponding local density of states (LDOS) by evaluating $(I/V)dI/dV$ numerically.[19] The representative LDOS curves from the lower bend section of the tube are shown in Fig.

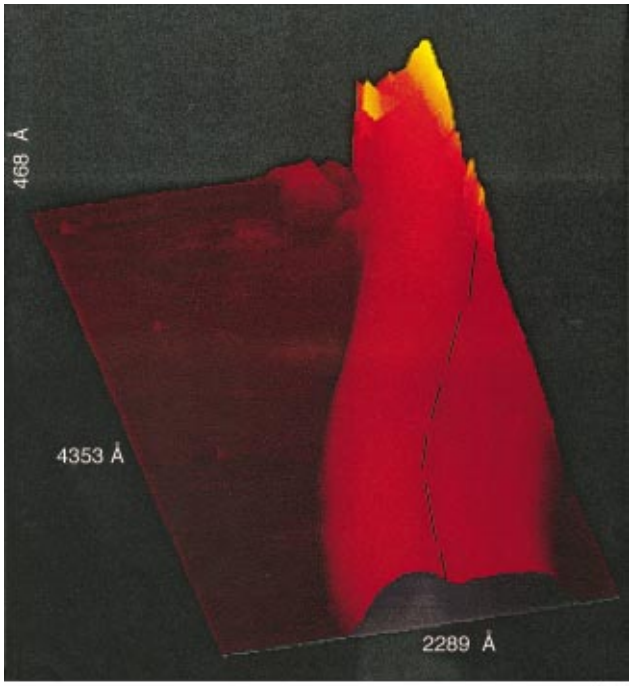

(a)

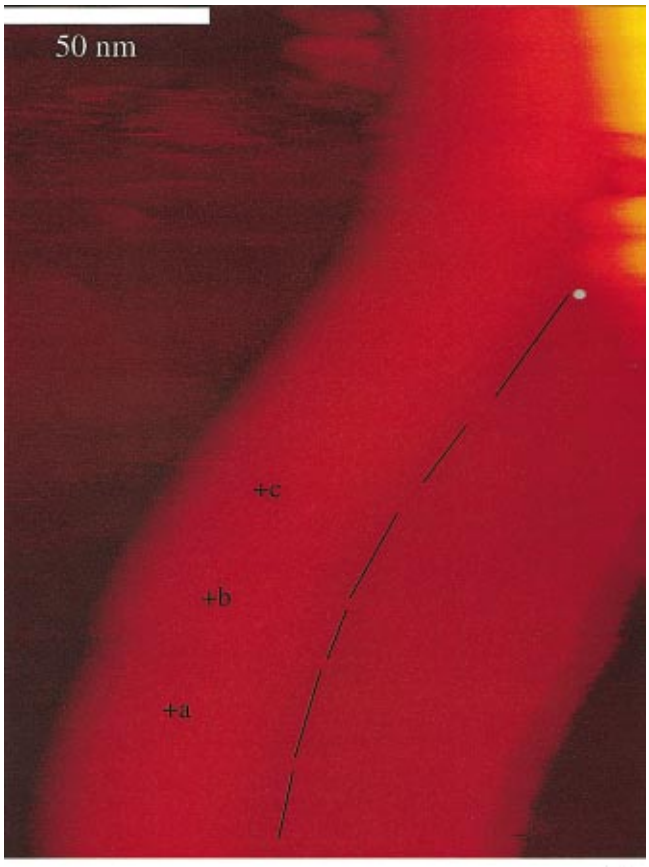

(b)

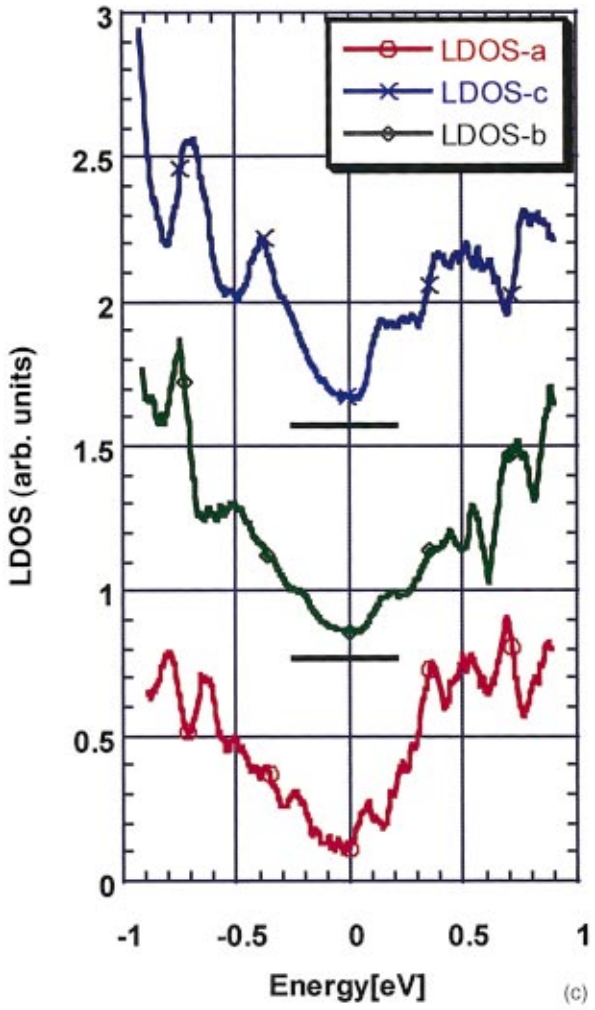

(c)

FIG. 1. (Color) (a) Three-dimensional (3D) STM image of tube $T1$ on the clean flat gold substrate. The Van der Waals forces and some amorphous carbon have held the tube fixed while it is bent. The region to the right of the dashed line is due to an imaging artifact. (b) Top view of tube $T1$ showing locations where spectroscopic measurements were taken from. The diameter of the tube is 12 nm$\pm$1 nm and the radius of curvature in the lower bend section is $\sim$300 nm making the tube to sustain a strain of $\sim$0.02. (c) LDOS curves of the tube $T1$ calculated from the measured I-V data. Each curve corresponds to the IV data collected from the locations marked $a-c$ in (a). These curves resemble one another suggesting that there is no significant electronic structure change due to the small strain.

1(c), where the letters $a-c$ correspond to the positions marked $a-c$ in Fig. 1(b). From the LDOS curves the tube appears to be metallic, with no significant variation in the width of the plateau ($\sim$0.1 eV$\pm$0.02 eV) near the Fermi energy.[20] The relative population of the density of states near the Fermi energy is also the same at the three locations. This suggests that no metal-insulator transition can be achieved due to small elastic strain on the tube. Furthermore, some of the Van Hove singularities occur near the same energy for the three curves. For example, see the maxima at $\sim\pm$0.8 eV in the LDOS plots. The LDOS features near $\sim+$0.5 eV are also similar. Such substantial similarities in the experimental results suggest that there are no significant changes in the electronic properties of the tube due to the small tensile strain it has sustained. This is well in agreement with the theoretical studies of Heyd *et al.*[11]

To compare the small strain effect with the large strain effect we have studied the electronic properties of a tube that is under high tensile strain due to its location on the substrate. Figure 2(a) is a STM image of a MWNT($T2$) (diameter 2.8 nm$\pm$0.1 nm) lying across a gold grain boundary. The tube appears to be bulged in regions *B* and *C* with more bulging in region *C*. Topographic view on the side parallel to the length of the tube shows that there is a height difference of $\sim$0.9 nm$\pm$0.1 nm between the grain domains on which the tube is located. The grain near the tube end marked *A* is at a lower level than the grain near the tube end marked *E*. Due to the van der Waals attraction, the tube tends to follow the substrate morphology, which causes it to be strained in regions around *B* and *C*. The region over which the tube is draped on the grain boundary is small making the tube highly strained ($\sim$13–18 %). Tunneling spectra from locations $A-E$ were used to calculate the LDOS as described before. The spectra from *A*, *D*, and *E* show that the tube is a semiconductor with a band gap of $\sim$0.4 eV$\pm$0.1 eV [see Fig. 2(b)]. The band gap of the tube has increased by a factor of about two at position *C* but it has reduced to nothing at position *B*. Furthermore, the density of states near the Fermi energy is higher at position *B* compared to other locations on the tube. The increase in DOS in the gap is an indication that the tube has metallic character in region *B*. Thus, the tube forms a *S-M-S* junction or a *quantum dot*.

The observed variation in the band gap of the tube can be explained in terms of the strain the tube experiences at region *C*. The tube must be stretched near region *C* to make up for the bend. Such extension, in effect, results in increasing the band gap of the tube.[11] Clearly, the tube is experiencing compression (on the side facing the substrate) in region *B* leading to a reduced band gap. However, there is more than a band gap narrowing in region *B*; the relative population of the density of states near the Fermi energy has also increased making the tube to behave metallic in the region. The question of how the tube gained its metallic property can be explained by analyzing three possible causes: (i) elastic shape deformation of the tube, (ii) presence of any defect states, and (iii) strain-caused chirality change. The first possibility can be excluded based on the fact that elastic deformations are known to lower the symmetry of the nanotubes.[6,8] The semiconducting tubes have lower symmetry than metallic tubes, and further symmetry lowering in semiconducting tubes is therefore unlikely to cause a change

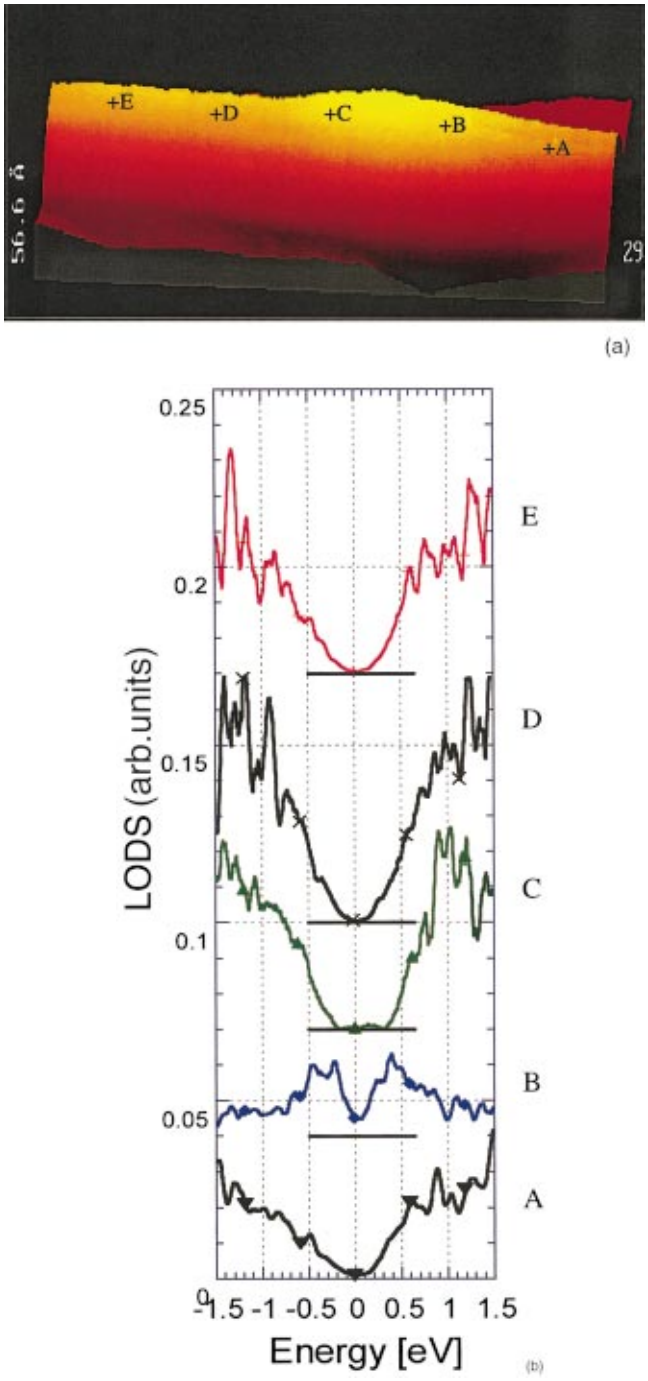

FIG. 2. (Color) (a) 3D image of tube $T2$ showing the deformation in the grain boundary. A height difference of $\sim$0.9 nm exists between the grain domains, making the tube to bend as it follows the morphology of the substrate. The letters $A-E$ show locations on the tube from which I-V data were collected. (b) LDOS curves of tube $T2$. Three distinct electronic property features are noted within a short segment of the tube: semiconducting-type LDOS (regions *A*, *D*, and *E*), metallic-type LDOS (region *B*), and wider band-gap semiconducting behavior (region *C*).

from semiconducting to metallic property. The metallic property is also not due to defect states. Since defect states appear only at specific energy levels[5,21,22] the resulting LDOS curve would be asymmetric relative to the Fermi energy. However, the observed LDOS in region *B* is symmetric relative to the Fermi energy. This excludes the second possibility and leaves the third possibility as the most probable mechanism by which the tube gains the observed heterogeneous electronic property.

A bending deformation generally creates local compressive and tensile strain on the in and out sides of the bend, respectively. For a hollow single-wall cylinder, bending is not expected to produce enough strain to cause atomic rearrangement. The reconfiguration is precluded by elastic buckling, which occurs earlier at approximately (Ref. 23) $\varepsilon_c = 0.08\,\mathrm{nm/d} < 0.03$, for the tube of 2.8 nm diam. However, in the case of multiwall nanotubes, for the outermost shell inward buckling is prevented by the inner layers, and much higher in-plane strain can be achieved, exceeding the thermodynamically critical value $\varepsilon_c = 0.06$, and thus causing a ''plastic'' response in the form of bond rotations.[12–14] Further, the change of chirality from chiral to achiral tube caused by mechanically induced Stone-Wales bond rearrangement can only occur under compressive, not tensile load. Indeed, the most energetically favorable bond rotation under axial compressive strain [Fig. 3(a)] creates a dislocation dipole 5/7/7/5 with the Burgers vectors $b = \pm(0,1)$. Further repetition of the similar transformations causes the 5/7 dislocations to dissociate and glide parallel to the line in opposite directions as indicated by the arrow lines in Fig. 3(a). This process results in a unit-index change $(n,n-1) \rightarrow (n,n)$ in the middle segment of the initial chiral $(n,n-1)$ tube. To approximately fit the observed 2.8-nm diam tube, we assign $n = 20$ and perform an evolution of this structure computationally, with the classical Tersoff-Brenner potential. The resulting relaxed configuration, shown in Fig. 3(b) satisfies the overall geometry requirements. It has initial semiconductor segments (20,19) at the two ends and metallic segment (20,20) in the middle, which results from a natural plastic-relaxation evolution under compression of a bent nanotube. This leads to the formation of a *S*-*M*-*S* junction with atomic structure of (20, 19)/(20, 20)/(20, 19), similar to the experimentally observed geometric and electronic properties of *T*2. The similarity can be further demonstrated by comparing Fig. 3(b) with the top view of *T*2 [Fig. 3(c)]. The compressive strain on the inner side of the bend can dissociate the dislocation dipoles inducing a change in helicity in the bend region of the tube [see Fig. 3(d)]. Thus, the observed electronic heterogeneity of *T*2 can be caused by the large compressive strain it experiences in region *B*. This simple model is intended to suggest only that such transformations due to strain lead naturally to observed results including the metallic local behavior and the conformational bulge.[24]

In summary, we have studied the effect of strain on the local electronic structure of the multiwall carbon nanotubes. No electronic property change is observed on the tube under small strain. In contrast, the tube under high strain due to

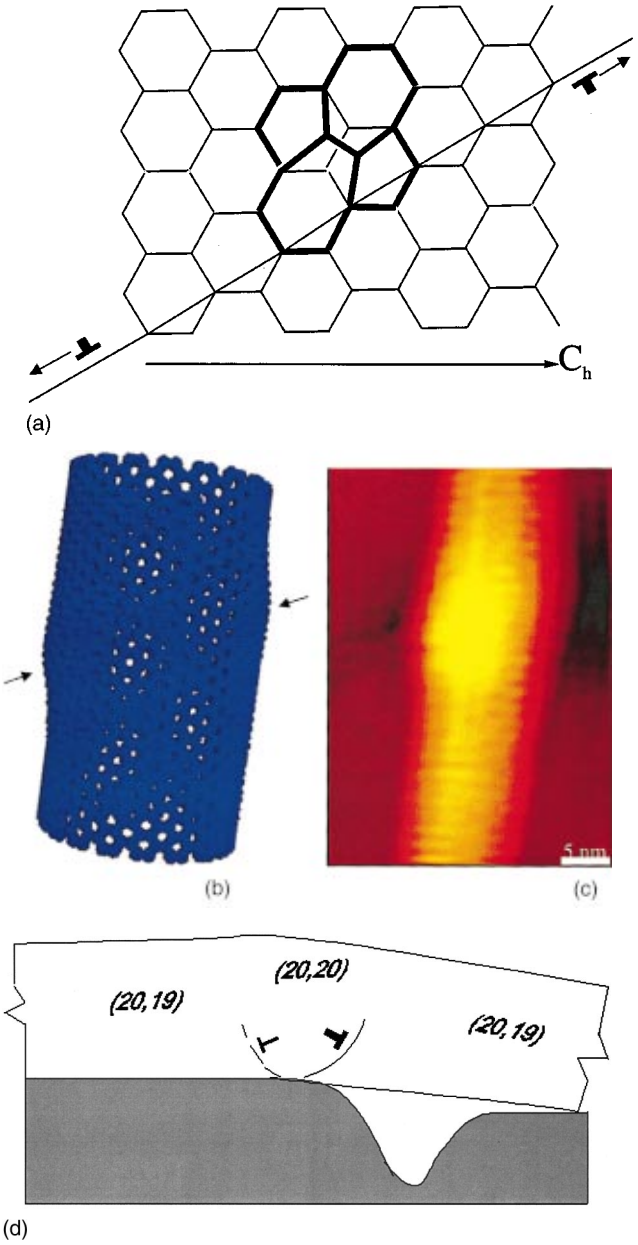

FIG. 3. (Color) (a) Schematics showing dislocation dipoles originated due to bond rotation while a compressive force is applied perpendicular to the chiral vector C_h. Successive bond rotations lead to the dissociation of the 5/7 defects resulting in local chirality change. The two small arrows indicate the direction in which the defects propagate. Computationally generated geometry of a tube that has semiconducting properties (20,19) at the two ends and a metallic property (20,20) in between. The dissociated 5/7 defects are located on the backside of the figure. The arrows indicate the positions along which the defects are found. The tube has metallic character in the segment between the two arrows. Top view (STM image) of tube T2. Its geometric and electronic property resemblance with (b) is striking. Schematic drawing showing the mechanical deformation of tube T2. The curved thin lines near the bend indicate the glideline of the 5/7 defects.

abrupt substrate morphology change, showed drastic change in the local electronic structure of the tube. Using classical molecular dynamics we have generated atomic structure that reproduces the observed geometry, ''force history'' and the electronic heterogeneity of the tube. Our results establish possible evidence of the effect of mechanics on the electrical properties of nanotubes.[24]

The authors D.T. and D.L.C. gratefully acknowledge financial support from NSF, and support for G.G.S. and B.I.Y. from AFRL/AFOSR and NASA Ames Center

[1] M. M. T. Treacy, T. W. Ebbesen, and J. M. Gibson, Nature (London) **381**, 678 (1996).
[2] W. Mintmire, B. I. Dunlap, and C. T. White, Phys. Rev. Lett. **68**, 631 (1992).
[3] N. Hamada, S. Sawada, and A. Oshiyama, Phys. Rev. Lett. **68**, 1579 (1992).
[4] R. Saito *et al.*, Appl. Phys. Lett. **60**, 2204 (1992).
[5] D. Tekleab *et al.*, Appl. Phys. Lett. **76**, 24 (2000).
[6] Chan-Jeong Park, Yong-Hyun Kim, and K. J. Chang, Phys. Rev. B **60**, 10 656 (1999).
[7] Alain Rochefort *et al.*, Phys. Rev. B **60**, 13 824 (1999).
[8] C. L. Kane and E. J. Mele, Phys. Rev. Lett. **78**, 1932 (1997).
[9] A. Bezryadin *et al.*, Phys. Rev. Lett. **80**, 4036 (1998).
[10] S. Paulso *et al.*, Appl. Phys. Lett. **75**, 2936 (1999).
[11] R. Heyd, A. Charlier, and E. McRae, Phys. Rev. B **55**, 6820 (1997).
[12] B. I. Yakobson, Appl. Phys. Lett. **72**, 918 (1998).
[13] M. Buongiorno Nardelli, B. I. Yakobson, and J. Bernholc, Phys. Rev. Lett. **81**, 4656 (1998).
[14] M. Buongiorno Nardelli, B. I. Yakobson, and J. Bernholc, Phys. Rev. B **57**, R4277 (1998).
[15] F.-X. Zha *et al.*, Phys. Rev. B **61**, 4884 (2000).
[16] Z. Yao *et al.*, Nature (London) **402**, 273 (1999).
[17] Jie Han *et al.*, Phys. Rev. B **57**, 14 983 (1998).
[18] M. S. C. Mazzani and H. Chacham, Phys. Rev. B **61**, 7312 (2000).
[19] The LDOS is calculated using the method developed in J. A. Stroscio and R. M. Feenstra, *Methods of Experimental Physics* (Academic, New York, 1993), Vol. 27.
[20] D. Tekleab, R. Czerw, D. L. Carroll, A. Rubio, and P. M. Ajayan (unpublished).
[21] L. Chico *et al.*, Phys. Rev. Lett. **76**, 6971 (1996).
[22] M. Menon and D. Srivastava, Phys. Rev. Lett. **79**, 4453 (1997).
[23] B. I. Yakobson, C. J. Brabec, and J. Bernholc, Phys. Rev. Lett. **76**, 2511 (1996).
[24] B. I. Yakobson, Physical Property Modification of Nanotubes, U.S. Patent, allowed for issuance, 2001.